

Organophosphoryl derivatives of trivacant tungstophosphates of general formula α -A-[PW₉O₃₄(RPO)₂]⁵⁻: synthesis and structure determination by multinuclear magnetic resonance spectroscopy (³¹P, ¹⁸³W) ‡

Cédric R. Mayer and René Thouvenot *†

Laboratoire de chimie des métaux de transition, URA CNRS 419, case 42, Université Pierre et Marie Curie, 4 place Jussieu, F75252 Paris cedex 05, France

In the presence of NBuⁿ₄Br acting as phase-transfer reagent, organophosphonic acids RPO(OH)₂ reacted in acetonitrile with the trivacant tungstophosphate sodium salt β-A-Na₈[HPW₉O₃₄]·24H₂O to give hybrid organophosphoryl polyoxotungstate derivatives α-A-[NBuⁿ₄]₃Na₂[PW₉O₃₄(RPO)₂] (R = Et **1**, Bu^t **2**, Buⁱ **3**, allyl **4** or Ph **5**) in satisfactory yield (>65%). The structure of the hybrid anions has been inferred from spectroscopic data, especially from multinuclear (³¹P, ¹⁸³W) NMR studies. In particular, the five-line (1:2:2:2:2) ¹⁸³W spectrum indicates a lowering of the symmetry of the tungstophosphate framework from C_{3v} to C_s. According to spectroscopic observations and chemical analyses, the hybrid anion consists of an α-A-[PW₉O₃₄] framework on which are grafted two RPO groups through P–O–W bridges. This structure displays two nucleophilic oxygen atoms at the polyoxotungstate surface and thus remains unsaturated.

Derivatized polyoxometalates (POMs) have received increasing attention for the last twenty years owing to their potential in bifunctional catalysis.² It has been recognized for a long time that the versatility of the polyoxometalates and their catalytic applications can be significantly increased by grafting organic and organometallic groups onto the polyoxometalate surface.

Our group is currently engaged in the systematic investigation of the reactivity of organohalogenosilanes SiRX₃ towards plurivacant polyoxotungstates.^{1,3} For example the trivacant Keggin tungstate anions [XW₉O₃₄]ⁿ⁻ (X = Si^{IV} or Ge^{IV}, n = 10; X = P^V or As^V, n = 9) yield organosilyl derivatives such as [XW₉O₃₄(Bu^tSiOH)₃]⁽ⁿ⁻⁶⁾⁻ and [XW₉O₃₄(RSiO)₃(RSi)]⁽ⁿ⁻⁶⁾⁻. Similarly, [AsW₉O₃₃(Bu^tSiOH)₃]³⁻ is obtained from the trivacant species B-[HAS^{III}W₉O₃₃]¹⁸⁻. All these hybrid anions are built up on the polyoxometalate surface which becomes saturated by formation of six Si–O–W bridges connecting three organosilyl groups RSi (Fig. 1). By an appropriate choice of the organic part, e.g. with the help of polymerizable groups or by setting up coupling reactions, one can conceive the easy synthesis of polyoxometalate-based interconnected networks which could give rise to polymeric hybrid organic–inorganic materials.

The reactivity of polyvacant polytungstates with organochlorostannanes was systematically investigated by Pope and co-workers⁴ because of the preference of tin for six-coordination, the structures of organotin derivatives are different from those of organosilyl hybrids, for example in [β-A-(PW₉O₃₄)₂(PhSnOH)₃]^{12-4a} and [α-A-(SiW₉O₃₄)₂(BuSnOH)₃]^{14-4b} three organostannyl groups are embedded in between two 9-tungsto anions.

To the best of our knowledge, the reaction of polyvacant polytungstates with organophosphonic acids has not yet been investigated. Except for a unique study of Kim and Hill⁵ on PhPO derivatives of monovacant tungsto-phosphate and -silicate, the other reported RPO derivatives of POMs were obtained by self-assembly processes and present some new structural arrangements.⁶ The present paper reports the synthesis and spectroscopic study of RPO derivatives of the trivacant tungstophosphate [PW₉O₃₄]⁹⁻. The structural charac-

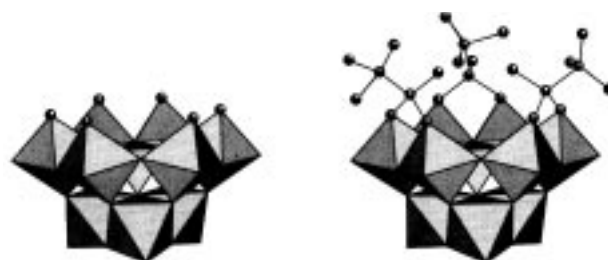


Fig. 1 Polyhedral representations of [PW₉O₃₄]⁹⁻ and [PW₉O₃₄(Bu^tSiOH)₃]³⁻

terization of these new species is achieved through a detailed multinuclear NMR investigation (³¹P, ¹⁸³W) in solution.

Results

A suspension of powdered β-A-Na₈H[PW₉O₃₄]·24H₂O⁷ in an acetonitrile solution of organophosphonic acid RPO(OH)₂ (R = Et, Bu^t, Buⁱ, allyl or Ph) and tetra-*n*-butylammonium bromide NBuⁿ₄Br was acidified with hydrochloric acid. After filtration and subsequent evaporation to dryness a white solid was obtained which was recrystallized from dimethylformamide (dmf). The compounds were characterized in the solid state by infrared spectroscopy and in solution by multinuclear magnetic resonance. Elemental analyses are consistent with the formula [NBuⁿ₄]₃Na₂[PW₉O₃₄(RPO)₂]·*x*dmf (R = Et **1**, Buⁿ **2**, Bu^t **3**, allyl **4** or Ph **5**; *x* = 0, 0.5 or 1).

Infrared characterization

The infrared spectra of all the compounds are very similar. A representative spectrum of **5** is shown in Fig. 2 and all data are given in Table 1. The low-wavenumber part ($\tilde{\nu} < 1000 \text{ cm}^{-1}$) is characteristic of the polyoxometalate framework.⁸ The stretching vibrational bands [$\nu_{\text{asym}}(\text{W}-\text{O}_\text{b}-\text{W})$ and $\nu_{\text{asym}}(\text{W}=\text{O}_{\text{ter}})$] are shifted to higher frequency, compared to those of the starting trivacant [PW₉O₃₄]⁹⁻ anion (Table 1). This effect, previously observed for organosilyl derivatives of trivacant polyoxotungstates,^{1,3} is attributed to a partial saturation of the polyoxometallic moiety through the fixation of RPO units. Moreover, the pattern of the 400–300 cm⁻¹ region is

† E-Mail: rth@ccr.jussieu.fr

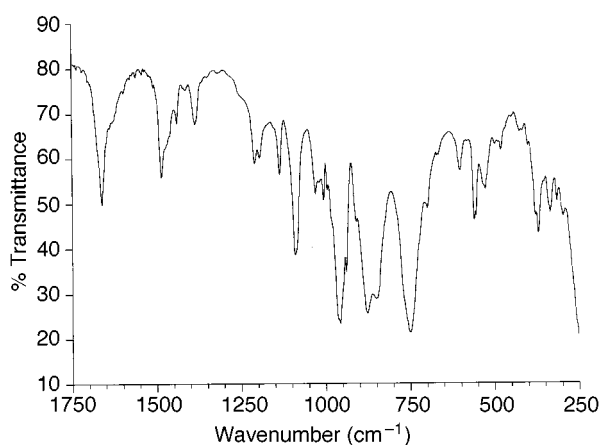
‡ Organic–inorganic hybrids based on polyoxometalates. Part 3.¹

Table 1 Infrared data (cm^{-1}) for $[\text{NBu}^n_4]_3\text{Na}_2[\text{PW}_9\text{O}_{34}(\text{RPO})_2]$ and $\beta\text{-A-Na}_8\text{H}[\text{PW}_9\text{O}_{34}]\cdot 24\text{H}_2\text{O}$

Assignment ^a	R					
	Et	Bu ⁿ	Bu ^t	Allyl	Ph	$\beta\text{-PW}_9$
$\nu(\text{P-C})$	1153w	1153w	1175w	1155w	1134w	
$\nu_{\text{asym}}(\text{P-O})^b$	1091s	1091s	1090s	1090s	1089s	1056s
	1026m	1023m	1034m	1024m	1029w	1014w
$\nu_{\text{asym}}(\text{P-O})^c$	1005m	1002m	1012m	1002m	1004w	
$\nu_{\text{asym}}(\text{W=O}_{\text{ter}})$	958vs	959vs	955vs	959vs	957vs	931vs
$\nu_{\text{asym}}(\text{W-O}_b\text{-W})$	877vs	877vs	878vs	877vs	877vs	821vs
	859vs	858vs	858vs	857vs	850vs	737vs
	750vs	751vs	747vs		750vs	
$\delta_{\text{asym}}(\text{O-P-O})$	600vw	596vw	601vw	601vw	601w	511w
	523m	527m	527m	522w	527w	
$\delta_{\text{asym}}(\text{W-O}_b\text{-W})$	377m	378m	379m	376m	377m	
	367m	369m	367m	367m	369m	363w
	330w	326w	333w	333w	334w	330m

^a Ref. 8. ^b PO_4 . ^c RPO .**Table 2** The ^{31}P NMR data^a for $[\text{PW}_9\text{O}_{34}(\text{RPO})_2]^{5-}$ anions

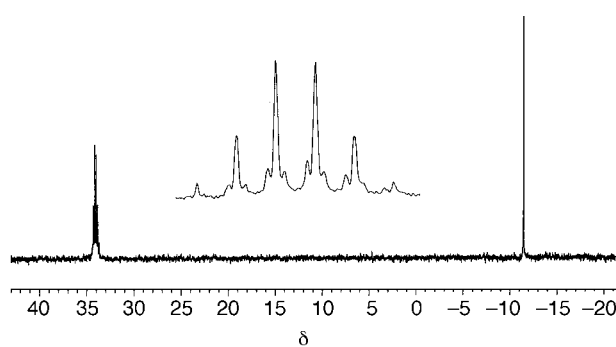
	R					Relative intensity ^b
	Et	Bu ⁿ	Bu ^t	Allyl	Ph	
PW_9O_{34}	-11.36	-11.26	-11.23	-11.51	-11.66	1
RPO	34.23	33.37	36	27.33	17.82	2
	(7.9)	(7.9)	(7.6)	(7.9)	(8.5)	

^a Chemical shifts in ppm relative to 85% H_3PO_4 . ² $J(\text{WP})$ in Hz in parentheses. ^b Measured on fully relaxed undecoupled spectra.**Fig. 2** Part of the IR spectrum ($\tilde{\nu} < 1750 \text{ cm}^{-1}$) of $[\text{NBu}^n_4]_3\text{Na}_2[\text{PW}_9\text{O}_{34}(\text{PhPO})_2]$

characteristic of the α isomer of the PW_9O_{34} unit.⁹ The stretching vibration bands of the PO_4 and RPO_3 groups are observed between 1000 and 1100 cm^{-1} . As for the W-O modes, the high-frequency shift of the $\nu_{\text{asym}}(\text{PO}_4)$ modes is indicative of the partial saturation of the polyoxometalate.

^{31}P NMR characterization

Each ^{31}P NMR spectrum presents two lines with a relative intensity of 2:1 (Fig. 3). Integration was carried out on proton-coupled spectra, with interpulse delays allowing full relaxation of the nuclei. The high-frequency resonance, with the expected multiplicity according to R (see Fig. 3), is attributed to the RPO group. This line displays satellites due to heteronuclear coupling [$^2J(\text{WP}) \approx 8 \text{ Hz}$, Table 2], which are most visible under proton-decoupling conditions. Integration of these satellites with respect to the central line¹⁰ shows that the P atom is connected to two tungsten atoms of the polyoxotungstate framework. The low-frequency singlet ($\delta -11.46 \pm 0.2$ for all R) of relative intensity 1 is assigned to the central PO_4 unit of the polyoxotungstate.⁷ This chemical shift, which is intermediate between

**Fig. 3** Proton-coupled ^{31}P NMR spectrum of a mother solution of $[\text{NBu}^n_4]_3\text{Na}_2[\text{PW}_9\text{O}_{34}(\text{EtPO})_2]$ (pulse angle 25° , acquisition time 0.8 s, relaxation delay 5 s) with expansion of the high-frequency line showing the tungsten satellites

that of the starting anion $[\text{PW}_9\text{O}_{34}]^{9-}$ ($\delta -5$, in the solid state)¹¹ and that of $[\text{PW}_9\text{O}_{34}(\text{Bu}^t\text{SiOH})_3]^{3-}$ ($\delta -15.9$),¹ is in accordance with a partially saturated tungstophosphate structure.

^{183}W NMR characterization

The ^{183}W NMR spectra of all species exhibit the same 1:2:2:2:2 pattern, consistent with C_s symmetry of the PW_9O_{34} framework (Fig. 4). All the signals present several satellites due to homonuclear tungsten-tungsten couplings. However, because of overlapping of these satellites, the determination of the $^2J(\text{WW})$ coupling constants required broad-band ^{31}P decoupling in order to suppress the multiplicity (see below). The three high-frequency lines appear as doublets due to the small coupling [$^2J(\text{WP}) < 2 \text{ Hz}$] with the central phosphorus atom of the PW_9O_{34} unit (Table 3). The two remaining (low-frequency) signals appear as doublets of doublets (Fig. 5); the smaller coupling [$^2J(\text{WP}) \approx 1.5 \text{ Hz}$] is similar to the previous one and the stronger coupling (6–9 Hz) corresponds to the μ -oxo junction W-O-P with the phosphorus atom of the RPO groups. For all species, the most shielded signal presents a significantly larger coupling (8–9 Hz) than the other one (6–8.5 Hz) (Table 3). These values are consistent with those observed by ^{31}P NMR spectroscopy (see above). Assignment of heteronuclear couplings was confirmed by selective ^{31}P decoupling experiments: by irradiating at the resonance frequency of the phosphonate group both low-frequency signals become doublets [keeping the small coupling $^2J(\text{WP}) \approx 1.5 \text{ Hz}$] while the other signals are unchanged.

Discussion

Syntheses

The trivacant polyoxotungstate $\beta\text{-A-}[\text{PW}_9\text{O}_{34}]^{9-}$ reacts readily

Table 3 The ^{183}W NMR data ^a for $[\text{PW}_9\text{O}_{34}(\text{RPO})_2]^{5-}$ anions

Assignment ^b	R					Relative intensity
	Et	Bu ⁿ	Bu ^t	Allyl	Ph	
W(1)	-42.8	-41.5	-44.2	-39.9	-40.4	1
W(6),W(7)	-94.6	-94.1	-96.8	-93.9	-92.5	2
W(2),W(3)	-140.0	-138.5	-141.6	-137.6	-138.6	2
W(4),W(9)	-189.0	-190.8	-180.0	-191.3	-191.1	2
	(6.1)	(6.6)	(6.4)	(7.1)	(8.5)	
W(5),W(8)	-193.8	-193.3	-190.4	-192.3	-192.9	2
	(7.9)	(8.0)	(7.9)	(7.9)	(9.0)	

^a Chemical shifts in ppm, ² $J(\text{WP})$ in Hz in parentheses (only coupling with RPO). ^b Numbering of the atoms, corresponding to structure I of Scheme 1.

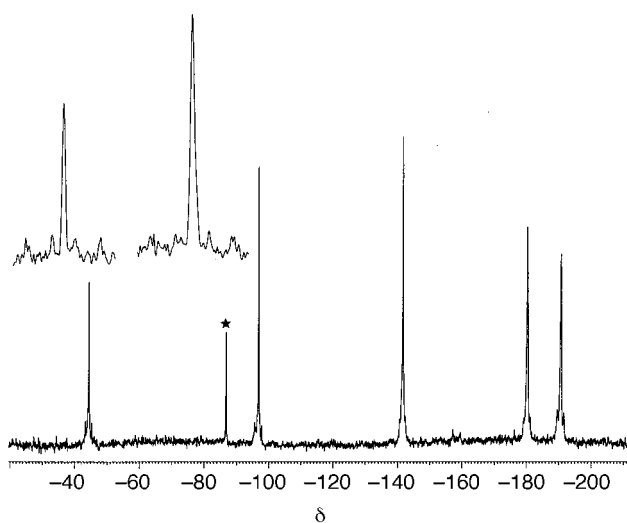
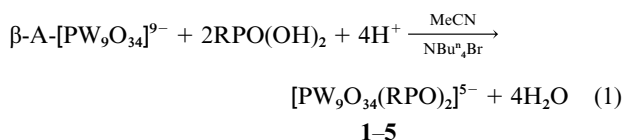


Fig. 4 A 12.5 MHz ^{183}W - $\{^{31}\text{P}\}$ NMR spectrum of $[\text{NBu}_4]_3\text{Na}_2[\text{PW}_9\text{O}_{34}(\text{Bu}^t\text{PO})_2]$ in $\text{dmf}-(\text{CD}_3)_2\text{CO}$ (0.3 M, pulse angle 90° ; acquisition time 1.64 s; number of scans 24 000; total acquisition time 11 h). The abscissa expansion of the δ -44.2 and -96.8 lines shows the tungsten satellites (digital resolution 0.15 Hz per point after 24 K points zero filling). The asterisk indicates $[\text{PW}_{12}\text{O}_{40}]^{3-}$ impurity

with electrophilic organophosphonic acids to yield hybrid organic-inorganic species $[\text{PW}_9\text{O}_{34}(\text{RPO})_2]^{5-}$. As for organochlorosilanes,^{1,3} the reaction with organophosphonates proceeds under phase-transfer conditions with NBu_4^+ acting as phase-transfer agent, equation (1). After filtration of a white



solid consisting of NaCl, NaBr and a small amount of unchanged sodium polyoxotungstate, the acetonitrile solution contains a single hybrid anionic species, as shown by ^{31}P NMR spectroscopy (see above), which has been isolated in high yield (ca. 70%) as its tetrabutylammonium salt. It can be recrystallized from a saturated dimethylformamide solution giving small well shaped plaquettes. Unfortunately all crystals (whatever R) appeared to be twinned and all our attempts to obtain suitable crystals for X-ray analyses (from other solvents and with other cations) were unsuccessful. The molecular structure of the hybrid anion is therefore derived from the spectroscopic results.

Infrared spectroscopy

The IR spectra of compounds 1-5 are nearly superimposable in the low-wavenumber ($\tilde{\nu} < 1000 \text{ cm}^{-1}$) region which is characteristic of the W-O stretching and bending vibrations.⁸ By comparison with $\beta\text{-A-Na}_8\text{H}[\text{PW}_9\text{O}_{34}] \cdot 24\text{H}_2\text{O}$, the vibrational bands of $[\text{NBu}_4]_3\text{Na}_2[\text{PW}_9\text{O}_{34}(\text{RPO})_2]$ appear relatively narrow, as is

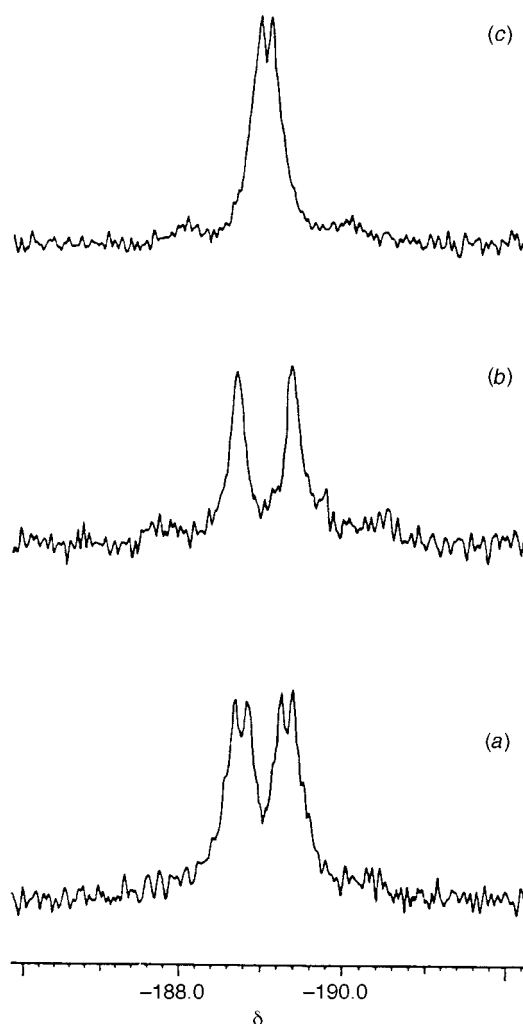
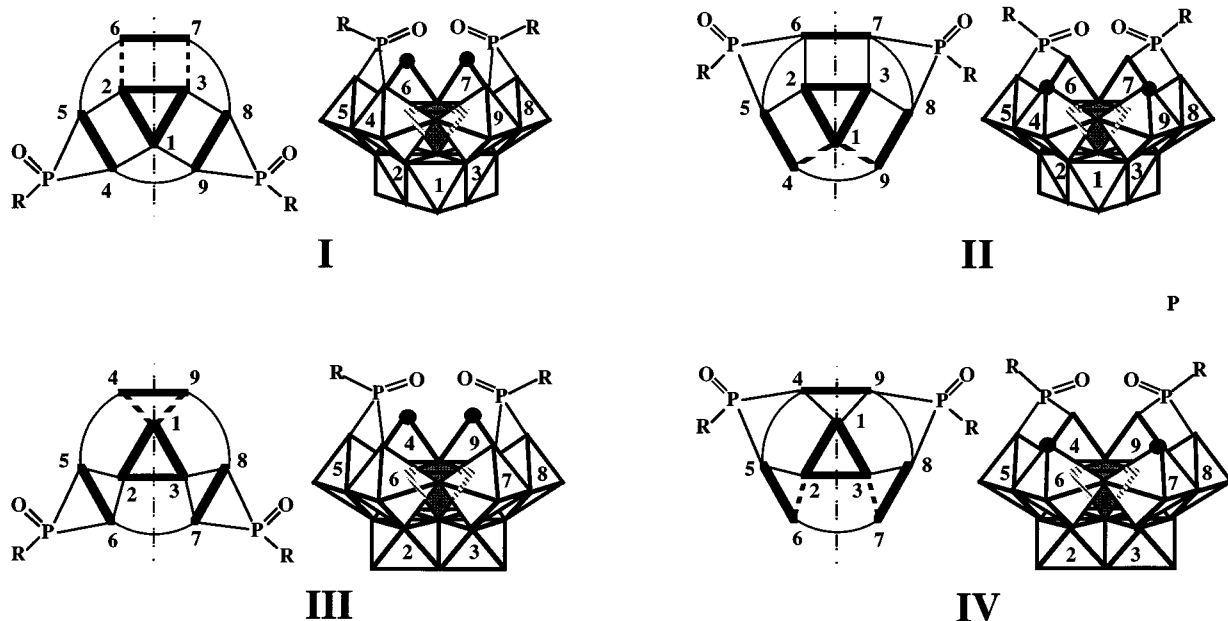


Fig. 5 Expansion of the δ -189 line of the 12.5 MHz ^{183}W NMR spectrum of $[\text{NBu}_4]_3\text{Na}_2[\text{PW}_9\text{O}_{34}(\text{EtPO})_2]$ in $\text{dmf}-(\text{CD}_3)_2\text{CO}$: (a) undecoupled, (b) selectively ^{31}P decoupled (irradiation at the PW_9O_{34} resonance) and (c) selectively ^{31}P decoupled (irradiation at the EtPO resonance)

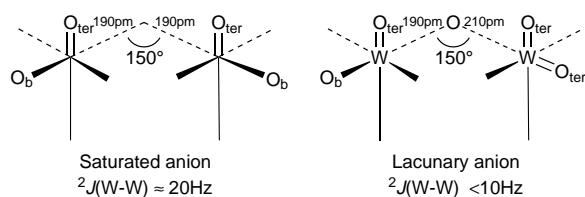
usually observed for tetrabutylammonium salts of polyoxometalates (Fig. 2).¹² Moreover the bands are shifted to higher wavenumbers which is indicative of saturation of the polyoxotungstate framework. In addition, it appears that the fixation of the phosphonate groups induces a $\beta \rightarrow \alpha$ isomerization of the PW_9O_{34} structure; this effect, deduced from the characteristic pattern in the $400\text{--}300 \text{ cm}^{-1}$ region,⁹ was also observed for organosilyl derivatives.^{1,3}

^{31}P NMR spectroscopy

The attachment of phosphonate groups onto the polyoxotungstate surface is demonstrated by the presence of tungsten



Scheme 1 Representation of the four possible structures for the $[\text{PW}_9\text{O}_{34}(\text{RPO})_2]^{5-}$ anion, based on α -A- PW_9O_{34} (I,II) and β -A- PW_9O_{34} (III, IV) units. For the polyoxotungstate framework in the plane representation, heavy and thin lines represent edge and corner junctions between adjacent octahedra respectively. The dashed lines correspond to peculiar corner junctions with expected low ${}^2J(\text{WW})$ coupling constants (*trans* influence)



Scheme 2 The *trans* influence and its consequences on homonuclear ${}^2J(\text{WW})$ coupling constants (O_{ter} = terminal oxygen, O_{μ} = μ -bridging oxygen)

satellites [${}^2J(\text{WP}) \approx 8$ Hz] around the high-frequency [$\delta + 18$ (5)–36 (3)] organophosphonate resonance. The relative intensity of these satellites with respect to the central line indicates that each RPO group is linked to two W atoms through two W–O–P bridges ($I_{\text{theor}} = 24.6$, $I_{\text{exp}} \approx 25\%$).¹⁰ Moreover the ${}^{31}\text{P}$ NMR spectra of compounds 1–5 are consistent with the grafting of only two phosphonate groups. Indeed, for all R, the integration of the phosphonate resonance with respect to the phosphate resonance indicates a ratio of two RPO groups per polyoxometalate, which is consistent with the chemical analysis. This result is rather surprising, as in the case of the organosilyl derivatives of PW_9O_{34} three RSi groups are simultaneously linked to the tungstophosphate framework. Partial ‘saturation’ of the polyoxotungstate surface in RPO derivatives is also revealed by the chemical shift of the PO_4 unit ($\delta - 11.5$) which is less shielded than in the ‘saturated’ organosilyl species $[\text{PW}_9\text{O}_{34}(\text{Bu}^t\text{SiOH})_3]^{3-}$ ($\delta - 15.9$).¹

${}^{183}\text{W}$ NMR spectroscopy

The ${}^{183}\text{W}$ NMR spectra of compounds 1–5 are also consistent with the loss of the ternary symmetry of the PW_9O_{34} framework. Actually, five lines (1:2:2:2:2) are observed for all organophosphonate derivatives which is in agreement with C_s symmetry for the PW_9O_{34} unit. Four different C_s structures can be considered (Scheme 1); two are based on a β -A- PW_9O_{34} moiety (III, IV) and two on a α -A- PW_9O_{34} moiety (I, II) with each RPO fragment linked either to a ditungsten group (I, III) or to two W atoms belonging to adjacent diads (II, IV).

All resonances have been assigned for the Bu^t derivative 3, with the following guideline: homonuclear tungsten–tungsten couplings ${}^2J(\text{WW})$ are less than 10 Hz for nuclei belonging to the same di- or tri-metallic group, and of the order of 20 Hz in

the other cases,¹³ except for W–O–W bridges *trans* to a $\text{W}=\text{O}_{\text{ter}}$ group [${}^2J(\text{WW}) < 10$ Hz].

The *trans* influence in polyoxotungstates. The first unambiguous assignment of ${}^{183}\text{W}$ NMR spectra of polyoxotungstates relied on the differences in homonuclear tungsten–tungsten coupling constants: indeed Brévard and co-workers^{13a} observed rather small ${}^2J(\text{WW})$ coupling constants (10 Hz or less) for edge junctions, with W–O–W angle of about 120° , with respect to corner junctions, with W–O–W about 145 – 150° [${}^2J(\text{WW}) \approx 20$ Hz]. It was shown later that more open μ -oxo bridges such as those in Dawson-type polyoxotungstates (W–O–W about 160°) display even larger coupling constants (≈ 30 Hz).¹⁴ This correlation between ${}^2J(\text{WW})$ and the W–O–W angle holds only for saturated polyoxotungstates, with nearly symmetrical W–O–W bridges (both W–O bonds ≈ 190 pm). In lacunary derivatives the W–O–W bridge *trans* to a $\text{W}=\text{O}_{\text{ter}}$ group is dissymmetrical, displaying a long W–O bond, in the range of 210–220 ppm (*trans* influence). Consequently, the coupling constant through the corresponding bridge is significantly reduced (Scheme 2).^{10,15} For example a corner-junction coupling as small as 4.9 Hz has been observed in the ${}^{183}\text{W}$ NMR spectrum of the divacant lacunary anion γ - $[\text{SiW}_{10}\text{O}_{36}]^{8-}$.¹⁵ The normal coupling constant is recovered by filling the lacuna.^{15b,16}

Assignments. The less-shielded resonance, with relative intensity one ($\delta - 41.3 \pm 1.3$), is unambiguously assigned to the tungsten atom W(1) lying in the plane of symmetry. Under ${}^{31}\text{P}$ decoupling (Fig. 4), two pairs of satellites, with two different homonuclear coupling constant values [${}^2J(\text{WW}) \approx 7.3$ and 24.4 Hz], are observed around this line. When considering the four different proposed structures (Scheme 1), in two of them (II, III) the W(1) atom is connected to W(4) [\equiv W(9)] which carries two terminal oxygen atoms. According to the *trans* influence, the corresponding coupling constant would be relatively low and W(1) should contract two small couplings. Thus, the exceptionally large value (24.4 Hz) is inconsistent with structures II and III. Only the two remaining structures I and IV may account for the large ${}^2J(\text{WW})$ constant, owing to the presence of a heteronuclear P–O–W bridge between the phosphonate group and the W(4) atom. Consistently the small coupling constant (7.3 Hz) corresponds to the W(1)–O–W(2) [\equiv W(1)–O–W(3)] bridge ($\alpha \approx 120^\circ$) in the trimetallic group.^{13a}

Table 4 The ^{183}W chemical shifts/coupling constants connectivity matrix for $[\text{PW}_9\text{O}_{34}(\text{Bu}^t\text{PO})_2]^{5-}$ *

	W(1)	W(6),W(7)	W(2),W(3)	W(4),W(9)	W(5),W(8)
W(1)	-44.2		7.5	24.4	
W(6),W(7)		-96.8	11.3		27
W(2),W(3)	7.3	11.3	-141.6		24.1
W(4),W(9)	24.4			-180.0	6.3
W(5),W(8)		27.6	24.4	6.7	-190.4

* Diagonal terms: chemical shifts, δ . Off-diagonal terms: $^2J(\text{WW})$ in Hz. Numbering of the atoms as in structure **I** of Scheme 1.

Unfortunately the other ^{183}W resonance lines appear relatively broad even under ^{31}P decoupling ($\Delta\nu_1 \approx 3\text{--}5$ Hz). This prevents an accurate determination of the small tungsten–tungsten couplings, as the corresponding satellites appear generally as shoulders at the foot of the central resonance. The large couplings are more easily observed: indeed, all four remaining lines present satellites with $^2J(\text{WW}) > 20$ Hz. However, a coupling constant of nearly the same value (24–25 Hz) is observed for three resonances. Thus, the assignment of W(4) [\equiv W(9)] is not possible on the basis of $^2J(\text{W}^1\text{W}^4) [\equiv ^2J(\text{W}^1\text{W}^9)] = 24.4$ Hz.

To proceed further with the assignment, we should consider the two most shielded resonances; they appear as doublets of doublets due to heteronuclear $^2J(\text{WP})$ couplings with the phosphorus atom of the PW_9O_{34} moiety ($J \approx 2$ Hz) and that of one RPO group ($J \approx 6\text{--}9$ Hz, depending on R). These lines should be assigned to the two pairs W(4) [\equiv W(9)] and W(5) [\equiv W(8)] of the structures **I** and **IV**. Under broad-band ^{31}P decoupling, the outermost line presents two pairs of tungsten satellites with large couplings [$^2J(\text{WW}) \approx 24$ (1W) and 27 Hz (1W)], whereas the second line exhibits only one pair of such satellites [$^2J(\text{WW}) \approx 24$ Hz (1W)] (Table 4, Fig. 4). Considering structure **IV** one would expect two strong couplings for both W(4) [\equiv W(9)] and W(5) [\equiv W(8)] pairs; therefore this structure can be ruled out and **I** remains as the only one consistent with the observed spectra. Consequently, the outermost line corresponds to W(5) and the second to W(4) with an observed homonuclear coupling constant [$^2J(\text{W}^1\text{W}^4) \equiv ^2J(\text{W}^1\text{W}^9) \approx 25$ Hz] consistent with the value (24.4 Hz) observed for the W(1) atom (see above).

Among the two remaining lines, the one at about $\delta -140$ clearly presents three pairs of satellites [$^2J(\text{WW}) \approx 7.5, \approx 11$ and 24.5 Hz] while that around $\delta -95$ exhibits only two pairs (even with resolution enhancement) (Fig. 4). The latter therefore corresponds to W(6) [\equiv W(7)], which is connected to W(5) through a strong coupling (≈ 27 Hz) and to W(2) [\equiv W(3)] through a medium coupling (≈ 11 Hz). For two tungsten nuclei belonging to corner-sharing octahedra ($\text{W}^1\text{--O}^1\text{--W}^2 \approx 150^\circ$), this relatively small coupling constant is consistent with the already mentioned *trans* influence (see above). Finally, assignment of the last line ($\delta -140$) to W(2) is consistent with the observed coupling constants $^2J(\text{W}^1\text{W}^2) [\equiv ^2J(\text{W}^1\text{W}^3)] = 7.3$, $^2J(\text{W}^2\text{W}^6) [\equiv ^2J(\text{W}^3\text{W}^7)] = 11.3$ and $^2J(\text{W}^2\text{W}^5) [\equiv ^2J(\text{W}^3\text{W}^8)] = 24.4$ Hz respectively.

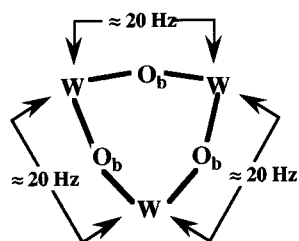
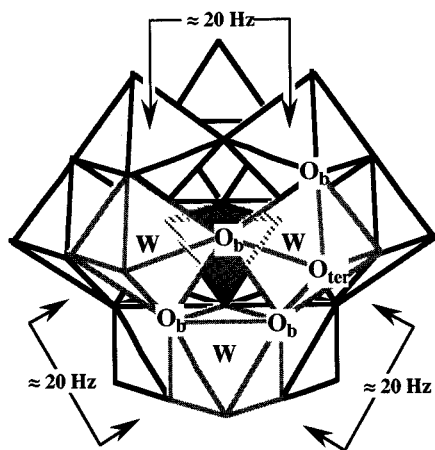
Heteronuclear $^2J(\text{WP})$ couplings. The heteronuclear $^2J(\text{WP})$ coupling constants follow a pattern similar to that of the homonuclear $^2J(\text{WW})$: the coupling constant through the μ -oxo bridge depends on the bridge angle and on both P–O and W–O distances. Mainly as a result of the long W–O bonds ($\approx 230\text{--}240$ pm) involving oxygen atoms of the central PO_4 tetrahedron, the corresponding coupling constants are generally small (less than 2 Hz). One should notice that the two resonances of the tungsten atoms belonging to the trimetallic group W(1)–W(3) display a particularly small coupling constant with the central phosphorus nucleus (<1 Hz) whereas this constant is significantly larger (≈ 2 Hz) for the three other resonances. Such a decrease of $^2J(\text{WP})$ through μ_n -O bonds with increasing n is

generally observed for phosphorus-centered Keggin and Dawson polyoxometalates.^{14,17}

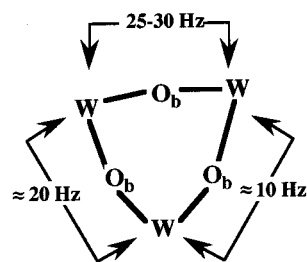
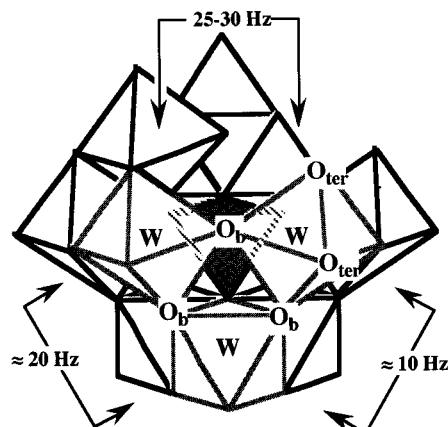
The phosphonate groups are connected to the polyoxotungstate framework through μ -O oxygen atoms. Therefore the $^2J(\text{WP})$ coupling constants along these bridges are relatively large, of the order of 6–9 Hz. However they remain significantly smaller than those observed by Kim and Hill⁵ for the phenylphosphonate derivatives of monovacant lacunary anions $[\text{PW}_{11}\text{O}_{39}]^{7-}$ and $[\text{SiW}_{11}\text{O}_{39}]^{8-}$ [$^2J(\text{WP})$ ranging from 15 to 30 Hz]. In the absence of any metrical parameter for our species, one can only speculate about the origin of these differences: although the anionic charge of the trivacant anion $[\text{PW}_9\text{O}_{34}]^{9-}$ is higher than that of the monovacant anion $[\text{PW}_{11}\text{O}_{39}]^{7-}$, the charge density is expected to be lower at each of the six oxygen atoms of the former species compared to the four oxygen atoms of the latter. Consequently the less nucleophilic O atoms of the trivacant anion should form weaker bonds with the phosphonate group. It should be noticed that a similar trend in heteronuclear coupling constants has been observed for organosilyl derivatives of lacunary polyoxotungstates: $^2J(\text{W}^1\text{--Si})$ is 6–7 Hz for the compounds derived from the trivacant anions α -A- $[\text{PW}_9\text{O}_{34}]^{9-}$ and α -A- $[\text{SiW}_9\text{O}_{34}]^{10-}$,¹³ whereas a coupling constant of 16.7 Hz has been reported for the vinylsilyl derivative of the monovacant tungstosilicate $[\text{SiW}_{11}\text{O}_{39}]^{8-}$.¹⁸

For $[\text{X}^{n+}\text{W}_{11}\text{O}_{39}(\text{PhPO})_2]^{(8-n)-}$ ($\text{X}^{n+} = \text{P}^{5+}$ or Si^{4+}) two coupling constants $^2J(\text{WP})$ of 14–15 and 26–27 Hz were reported, corresponding to two different P–O–W bridges, with tungsten atoms belonging either to a diad or to a triad.⁵ Two different coupling constants $^2J(\text{WP})$ are also observed for $[\text{PW}_9\text{O}_{34}(\text{RPO})_2]^{5-}$ (Table 3). However the differences are relatively small [$^2J(\text{W}^4\text{P}) = 6\text{--}8.5$, $^2J(\text{W}^5\text{P}) = 8\text{--}9$ Hz] and arise only in the ^{183}W NMR spectra. Indeed, according to the proposed structure, the bridge between the phosphonate group and the tungsten nuclei W(4) is not symmetrically related to that between the phosphonate group and the tungsten nuclei W(5). The different coupling constants $^2J(\text{WP})$ might reflect a slightly larger P–O–W angle or a shorter P–O bond in the (R)P–O–W(5) bridge than in the (R)P–O–W(4) bridge.

Homonuclear $^2J(\text{WW})$ couplings. As a result of the low symmetry of the $[\text{PW}_9\text{O}_{34}(\text{RPO})_2]^{5-}$ anions, different tungsten–tungsten coupling constants are observed in the ^{183}W NMR spectra. Compared to those of the organosilyl derivatives, the coupling constants involving the W atoms of the triad W(1)–W(3) and the tungsten atoms connected to the phosphonate are relatively large (25 compared to 22 Hz). The large coupling constants $^2J(\text{W}^5\text{W}^6) [\equiv ^2J(\text{W}^7\text{W}^8)]$ should be considered together with the smaller one $^2J(\text{W}^2\text{W}^6) [\equiv ^2J(\text{W}^3\text{W}^7)]$. Actually a redistribution of the homonuclear tungsten–tungsten coupling constants in the vicinity of a *cis*- WO_2 unit has been observed in any case of a small corner coupling induced by *trans* influence. For example, in the monovacant polyoxotungstate $[\text{SiW}_{11}\text{O}_{39}]^{8-}$ and polyoxomolybdotungstate $[\text{SiMo}_2\text{W}_9\text{O}_{39}]^{8-}$, the *cis*- WO_2 units display two peculiar corner-coupling constants: a small one (≈ 10 Hz) which involves the oxygen atom *trans* to O_{ter} and a large one (>25 Hz) (Scheme 3).^{15b,19} The same effect has also been observed in monovacant lacunary anions of the Dawson structure.²⁰



Saturated Keggin anion



Monovacant Keggin anion

Scheme 3 Comparison of ${}^2J(\text{WW})$ corner-coupling constants for saturated and monovacant lacunary Keggin polyoxotungstates^{15b,19}

In the present case, as for monovacant species, the redistribution of the homonuclear coupling constants might be interpreted by a geometrical rearrangement in the vicinity of the *cis*-WO₂ groups. As a consequence of the *trans* influence, the tungsten atom is markedly displaced from the centre of the WO₆ octahedron. Molecular models show that this might result in a relatively large W–O–W angle (>150°) for the second corner junction.

Conclusion

Despite all our efforts to grow suitable crystals of the RPO derivatives of [PW₉O₃₄]⁹⁻, no X-ray diffraction study was possible. Nevertheless the molecular structure of the hybrid anion can be confidently deduced from the spectroscopic data (Fig. 6). This anion consists of an α -A-PW₉O₃₄ unit on which are grafted two RPO groups through two P–O–W bridges. As for the analogous organosilyl derivatives, each RPO group is connected to two W atoms belonging to the same dimetallic unit (diad). However, contrary to organosilyl derivatives where the six nucleophilic oxygen atoms of the trivacant anion are saturated, the grafting of organophosphonates retains intact two oxygen atoms. Together with the two free oxygen atoms of the phosphonate groups, they define a new lacuna, for the binding of the two sodium cations revealed by chemical analysis. However the electrostatic interaction between Na⁺ and these oxygen atoms should be relatively weak so that the polyoxotungstate surface remains available to further electrophilic attack. Indeed the hybrid [PW₉O₃₄(RPO)₂]⁵⁻ anions react with trichloroorgano-silanes, -germanes and -stannanes to afford saturated derivatives. Work on this subject is in progress.

Experimental

General

The compound β -A-Na₈H[PW₉O₃₄] \cdot 24H₂O was prepared

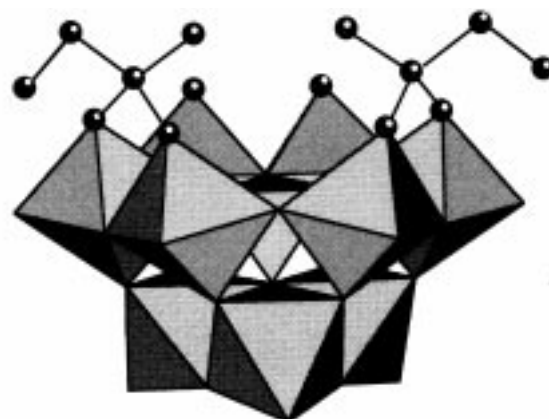


Fig. 6 Polyhedral representation of the proposed structure for [PW₉O₃₄(RPO)₂]⁵⁻ (R = Et)

according to the literature.⁷ Other reagents, [RPO(OH)₂ and NBu₄Br] and solvents were from Aldrich and used as received. Elemental analyses were performed by the Service central de microanalyses du CNRS, Vernaison, France.

The IR spectra (4000–250 cm⁻¹) were recorded on a Bio-Rad FTS 165 IR FT spectrometer with compounds sampled in KBr pellets, ¹³C (75.46) and ³¹P (121.5 MHz) NMR spectra at room temperature in 5 mm outside diameter tubes on a Bruker AC 300 spectrometer equipped with a QNP probehead. The chemical shifts are given according to the IUPAC convention, with respect to SiMe₄ and 85% H₃PO₄ respectively. The 12.5 MHz ¹⁸³W NMR spectra were recorded at 300 K on nearly saturated dmf-(CD₃)₂CO (90:10, v/v) solutions in 10 mm outside diameter tubes on the same spectrometer equipped with a low-frequency special VSP probehead. The chemical shifts are given with respect to 2 M Na₂WO₄ aqueous solution and were determined by the substitution method using a saturated D₂O solution of tungstosilicic acid H₄SiW₁₂O₄₀ as secondary standard

(δ –103.8). The ^{31}P decoupling experiments were performed with a B-SV3 unit operating at 121.5 MHz and equipped with a B-BM1 broad-band modulator. Selective or broad-band decoupling was determined by appropriate choice of the synthesizer frequency and of the output power (4–40 W) before entering the decoupling coil of the low-frequency probehead.

Preparations

α -A-[NBu n $_4$] $_3$ Na $_2$ [PW $_9$ O $_{34}$ (EtPO) $_2$] 1. The compounds β -A-Na $_8$ H[PW $_9$ O $_{34}$] \cdot 24H $_2$ O (11.5 g, 4 mmol) and NBu n $_4$ Br (4.62 g, 14 mmol) were suspended in MeCN (50 cm 3); EtPO(OH) $_2$ (0.88 g, 8 mmol) was added under vigorous stirring, then HCl (1.36 cm 3 , 16 mmol) was added dropwise and the mixture stirred overnight at reflux. After separation of a white solid (NaCl, NaBr + traces of Na $_8$ H[PW $_9$ O $_{34}$]), the white compound [NBu n $_4$] $_3$ Na $_2$ [PW $_9$ O $_{34}$ (EtPO) $_2$] was formed by evaporation of the resulting solution in a rotary evaporator. The crude compound was recrystallized from dmf. Yield: 8.5 g (67.5%) (Found: C, 20.22; H, 3.87; N, 1.30; Na, 1.34; P, 2.88, W, 51.10. Calc. for C $_{52}$ H $_{118}$ N $_3$ Na $_2$ O $_{36}$ P $_3$ W $_9$: C, 19.80; H, 3.77; N, 1.33; Na, 1.46; P, 2.95; W, 52.44%). δ_{C} (75.46 MHz, solvent acetone, standard SiMe $_4$) 22.73 [1C, d, $J(\text{PC})$ 147] and 7.25 [1C, d, $J(\text{PC})$ 6.49 Hz].

α -A-[NBu n $_4$] $_3$ Na $_2$ [PW $_9$ O $_{34}$ (Bu n PO) $_2$] \cdot dmf 2. This compound was similarly synthesized from β -A-Na $_8$ H[PW $_9$ O $_{34}$] \cdot 24H $_2$ O (11.5 g, 4 mmol), NBu n $_4$ Br (4.62 g, 14 mmol), Bu n PO(OH) $_2$ (1.1 g, 8 mmol) and HCl (1.36 cm 3 , 16 mmol). Yield: 8.9 g (67.4%) (Found: C, 21.12; H, 4.09; N, 1.74; Na, 1.36; P, 2.78; W, 49.75. Calc. for C $_{59}$ H $_{133}$ N $_4$ Na $_2$ O $_{37}$ P $_3$ W $_9$: C, 21.58; H, 4.08; N, 1.71; Na, 1.40; P, 2.83; W, 50.38%). δ_{C} (75.46 MHz, solvent acetone, standard SiMe $_4$) 27.90 [1C, d, $J(\text{PC})$ 146.5], 24.75 [1C, d, $J(\text{PC})$ 4], 23.0 [1C, d, $J(\text{PC})$ 7.1 Hz] and 12.65 (1C, s).

α -A-[NBu n $_4$] $_3$ Na $_2$ [PW $_9$ O $_{34}$ (Bu n PO) $_2$] \cdot 0.5dmf 3. This compound was similarly synthesized from β -A-Na $_8$ H[PW $_9$ O $_{34}$] \cdot 24H $_2$ O (11.5 g, 4 mmol), NBu n $_4$ Br (4.62 g, 14 mmol), Bu n PO(OH) $_2$ (1.1 g, 8 mmol) and HCl (1.36 cm 3 , 16 mmol). Yield: 9.0 g (68.1%) (Found: C, 21.14; H, 3.97; N, 1.43; Na, 1.41; P, 2.87; W, 51.16. Calc. for C $_{57.5}$ H $_{129.5}$ N $_{3.5}$ Na $_2$ O $_{36.5}$ P $_3$ W $_9$: C, 21.27; H, 4.02; N, 1.51; Na, 1.42; P, 2.86; W, 50.95%). δ_{C} (75.46 MHz, solvent acetone, standard SiMe $_4$) 33.04 [1C, d, $J(\text{PC})$ 148.3 Hz] and 26.29 (3C, s).

α -A-[NBu n $_4$] $_3$ Na $_2$ [PW $_9$ O $_{34}$ (C $_3$ H $_5$ PO) $_2$] \cdot 0.5dmf 4. This compound was similarly synthesized from β -A-Na $_8$ H[PW $_9$ O $_{34}$] \cdot 24H $_2$ O (11.5 g, 4 mmol), NBu n $_4$ Br (4.62 g, 14 mmol), C $_3$ H $_5$ PO(OH) $_2$ (0.98 g, 8 mmol) and HCl (1.36 cm 3 , 16 mmol). Yield: 8.3 g (65.4%) (Found: C, 20.81; H, 3.81; N, 1.49; Na, 1.41; P, 2.82; W, 50.16. Calc. for C $_{55.5}$ H $_{121.5}$ N $_{3.5}$ Na $_2$ O $_{36.5}$ P $_3$ W $_9$: C, 20.73; H, 3.81; N, 1.52; Na, 1.43; P, 2.89; W, 51.46%). δ_{C} (75.46 MHz, solvent acetone, standard SiMe $_4$) 131.1 [1C, d, $J(\text{PC})$ 10.6], 115.8 [1C, d, $J(\text{PC})$ 15] and 34.42 [1C, d, $J(\text{PC})$ 146.0 Hz].

α -A-[NBu n $_4$] $_3$ Na $_2$ [PW $_9$ O $_{34}$ (PhPO) $_2$] 5. This compound was similarly synthesized from β -A-Na $_8$ H[PW $_9$ O $_{34}$] \cdot 24H $_2$ O (11.5 g,

4 mmol), NBu n $_4$ Br (4.62 g, 14 mmol), PhPO(OH) $_2$ (1.26 g, 8 mmol) and HCl (1.36 cm 3 , 16 mmol). Yield: 9.2 g (71%) (Found: C, 21.79; H, 3.76; N, 1.27; Na, 1.39; P, 2.82; W, 49.96. Calc. for C $_{60}$ H $_{118}$ N $_3$ Na $_2$ O $_{36}$ P $_3$ W $_9$: C, 22.17; H, 3.66; N, 1.29; Na, 1.41; P, 2.86; W, 50.89%). δ_{C} (75.46 MHz, solvent acetone, standard SiMe $_4$) 136.5 [1C, d, $J(\text{PC})$ 147.5], 130.8 [2C, d, $J(\text{PC})$ 6], 129 (1C, s) and 127.72 [2C, d, $J(\text{PC})$ 9 Hz].

References

- 1 Part 2, A. Mazeaud, N. Ammari, F. Robert and R. Thouvenot, *Angew. Chem., Int. Ed. Engl.*, 1996, **35**, 1961; *Angew. Chem.*, 1996, **108**, 2089.
- 2 See, for example, M. T. Pope and A. Müller, *Angew. Chem., Int. Ed. Engl.*, 1991, **30**, 34; *Angew. Chem.*, 1991, **103**, 56; *Polyoxometalates: From Platonic Solids to Anti-Retroviral Activity*, eds. M. T. Pope and A. Müller, Kluwer, Dordrecht, 1994.
- 3 N. Ammari, G. Hervé and R. Thouvenot, *New. J. Chem.*, 1991, **15**, 607; N. Ammari, Ph.D. Thesis, Université Pierre et Marie Curie, Paris, 1993.
- 4 (a) F. Xin and M. T. Pope, *Organometallics*, 1994, **13**, 4881; (b) F. Xin, M. T. Pope, G. J. Long and U. Russo, *Inorg. Chem.*, 1996, **35**, 1207.
- 5 G. S. Kim and C. L. Hill, *Inorg. Chem.*, 1992, **31**, 5316.
- 6 P. R. Sethuraman, M. A. Leparulo, M. T. Pope, F. Zonnevillje, C. Brévard and J. Lemerle, *J. Am. Chem. Soc.*, 1981, **103**, 7665; U. Kotz, B. Jameson and M. T. Pope, *J. Am. Chem. Soc.*, 1994, **116**, 2659.
- 7 R. Massart, R. Contant, J.-M. Fruchart, J.-P. Ciabrini and M. Fournier, *Inorg. Chem.*, 1977, **16**, 2916.
- 8 C. Rocchiccioli-Deltcheff, R. Thouvenot and R. Franck, *Spectrochim. Acta, Part A*, 1975, **32**, 587.
- 9 R. Thouvenot, M. Fournier, R. Franck and C. Rocchiccioli-Deltcheff, *Inorg. Chem.*, 1984, **23**, 598.
- 10 R. Thouvenot, A. Tézé, R. Contant and G. Hervé, *Inorg. Chem.*, 1988, **27**, 524.
- 11 W. H. Knoth, P. J. Domaille and R. D. Farlee, *Organometallics*, 1985, **4**, 62.
- 12 C. Rocchiccioli-Deltcheff, M. Fournier, R. Franck and R. Thouvenot, *Inorg. Chem.*, 1983, **22**, 207.
- 13 (a) J. Lefebvre, F. Chauveau, P. Doppelt and C. Brévard, *J. Am. Chem. Soc.*, 1981, **103**, 4589; (b) P. J. Domaille, *J. Am. Chem. Soc.*, 1984, **106**, 7677.
- 14 R. Contant and R. Thouvenot, *Inorg. Chim. Acta*, 1993, **212**, 41.
- 15 (a) J. Canny, A. Tézé, R. Thouvenot and G. Hervé, *Inorg. Chem.*, 1986, **25**, 2114; (b) E. Cadot, R. Thouvenot, A. Tézé and G. Hervé, *Inorg. Chem.*, 1992, **31**, 4128.
- 16 A. Tézé, J. Canny, L. Gurban, R. Thouvenot and G. Hervé, *Inorg. Chem.*, 1996, **35**, 1001.
- 17 R. Acerete, C. F. Hammer and L. C. W. Baker, *J. Am. Chem. Soc.*, 1979, **101**, 267; R. Acerete, S. Harmaker, C. F. Hammer, M. T. Pope and L. C. W. Baker, *J. Chem. Soc., Chem. Commun.*, 1979, 777; R. Acerete, C. F. Hammer and L. C. W. Baker, *J. Am. Chem. Soc.*, 1982, **104**, 5384; *Inorg. Chem.*, 1984, **23**, 1478; M. Abbessi, R. Contant, R. Thouvenot and G. Hervé, *Inorg. Chem.*, 1991, **30**, 1695.
- 18 P. Judeinstein, C. Deprun and L. Nadjo, *J. Chem. Soc., Dalton Trans.*, 1991, 1991.
- 19 R. Contant, G. Hervé and R. Thouvenot, presented at the CNRS-NSF polyoxometalate workshop, St-Lambert des Bois, 1983.
- 20 R. Thouvenot and R. Contant, unpublished work.

Received 21st July 1997; Paper 7/05216B